RSC Advances

This is an *Accepted Manuscript*, which has been through the Royal Society of Chemistry peer review process and has been accepted for publication.

Accepted Manuscripts are published online shortly after acceptance, before technical editing, formatting and proof reading. Using this free service, authors can make their results available to the community, in citable form, before we publish the edited article. This *Accepted Manuscript* will be replaced by the edited, formatted and paginated article as soon as this is available.

You can find more information about *Accepted Manuscripts* in the Information for Authors.

Please note that technical editing may introduce minor changes to the text and/or graphics, which may alter content. The journal's standard Terms & Conditions and the Ethical guidelines still apply. In no event shall the Royal Society of Chemistry be held responsible for any errors or omissions in this *Accepted Manuscript* or any consequences arising from the use of any information it contains.

ROYAL SOCIETY OF CHEMISTRY

www.rsc.org/advances

Journal Name

RSC Advances

Dynamic Article Links ►

Cite this: DOI: 10.1039/c0xx00000x

www.rsc.org/xxxxxx

ARTICLE TYPE

RSC Advances Accepted Manuscript

$Al(CH_3)_3$-promoted Pt/MCM-41 catalysts for tetralin hydrogenation in the presence of benzothiophene and promotion mechanism of Al-promoted Pt/MCM-41 catalysts

Mingjian Luo,*[a,b] Qingfa Wang,[b] Xiangwen Zhang,[b] Li Wang,[b] Bing Hu[a]

Received (in XXX, XXX) Xth XXXXXXXXX 20XX, Accepted Xth XXXXXXXXX 20XX
DOI: 10.1039/b000000x

a. Provincial Key Laboratory of Oil & Gas Chemical Technology, College of Chemistry & Chemical Engineering, Northeast Petroleum University, Daqing 163318, P.R. China. E-mail: luomingjian@nepu.edu.cn, luomingjian@tju.edu.cn, Tel.: +86 459 6507736
b. Key Laboratory for Green Chemical Technology of Ministry of Education, School of Chemical Engineering and Technology, Tianjin University, Tianjin 300072, P.R. China. E-mail: qfwang@tju.edu.cn, Tel. /fax: +86 22 27892340

$Al(CH_3)_3$-promoted Pt-Al/MCM-41 catalysts with Al/Pt ratio from 0 to 20 were prepared for tetralin hydrogenation under sulfur-free and sulfur-containing condition. NH_3-TPD and Py-FTIR results indicate that the acid amount of catalyst increases with the increase of Al/Pt. The electron with-drawing effect of Al-promoter decreases the electron density of platinum particles and leads to the formation of electron deficient $Pt^{\delta+}$. The isolation effect of Al-promoter which benefits the platinum dispersion plays a leading role at low Al/Pt while the anchor effect which leads to large platinum particle dominates the high Al/Pt. The platinum dispersion increases at low Al/Pt and decreases at high Al/Pt. The catalyst with Al/Pt = 10 has the best platinum dispersion. All Al-promoted catalysts are much better tetralin hydrogenation activity and sulfur-tolerance than the Al-free one. Among which the one with Al/Pt = 10 is the best. The improvement in platinum dispersion is the primary factor that benefits both tetralin hydrogenation performance and sulfur-tolerance. However, tetralin hydrogenation prefers to less electron deficient platinum particle while the sulfur-tolerance is in favor of electron deficient $Pt^{\delta+}$.

1. Introduction

Reduction the aromatics in diesel fuel is an important process to increase the cetane number as well as reduce the emission of particulates, NOx and polycyclic aromatic hydrocarbons (PAH). [1] Hydrodearomatization processes are typically used for reducing the aromatic compounds. Contrast to the hydrodesulfurization and the hydrodenitrification, the reversible exothermal aromatic hydrogenation reaction is more favor of mild reaction temperature.[2, 3] Generally, the supported noble metal catalysts, which are high aromatic hydrogenation activity at mild reaction conditions, are used in the production of low aromatic diesel.[2-4] However, the activity of noble metal catalysts is dramatically suppressed by the presents of sulfur-containing and nitride-containing compounds in the feedstock.

Efforts have been paid on improving the sulfur-tolerance of noble metal of catalyst. It has been proved that the supports with suitable acidity have positive effects on the hydrodearomatization activity and sulfur-tolerance of noble-metals catalysts. [5-10] These effects have been attributed to the synergistic effects between acid sites and noble metal particles which leads to the formation of electron-deficient metal ($M^{\delta+}$),[9-11] the additional active sites provides by the acid sites and the hydrogen spillover between the acid sites and metal sites.[3, 12-14] For the better understand of the interaction between acid sites and noble metal particles, we have investigated the properties and the performances of $AlCl_3$, $Al(NO_3)_3$ and $Al(CH_3)_3$ promoted Pt/MCM-41 catalysts by post-synthesis alumination and found that: 1) For the $AlCl_3$ promoted catalysts, the pre-grafting $AlCl_3$ anchors the platinum around it and leads to the most electron-deficient $Pt^{\delta+}$, while grafting $AlCl_3$ after the support of platinum offers isolation effect which benefits the platinum dispersion as well as leads to the formation of electron-deficient $Pt^{\delta+}$.[15] 2) The electron density of platinum particles decreases with the increase of $AlCl_3$/Pt ratio, while the scale of platinum particles decreased first and then increased. [16] 3) Contrast to $Al(NO_3)_3$ and $AlCl_3$, the $Al(CH_3)_3$ has the best isolation effect and the electron-donating methyl group. Thus $Al(CH_3)_3$-promoted catalyst is better platinum dispersion and less electron-deficient than $Al(NO_3)_3$- and $AlCl_3$-promoted ones. [17] And 4) the tetralin hydrogenation is in favor of high platinum dispersion and less electron-deficient Pt particles while the sulfur-tolerance prefers electron-deficient $Pt^{\delta+}$.[15-17]

Due to its excellent promotion effect on the tetralin hydrogenation activity and sulphur-tolerance of Pt/MCM-41 catalyst, further investigation on the effects of Al/Pt ratio on the properties and performance of $Al(CH_3)_3$-promoted Pt/MCM-41 catalysts is performed in this work. The promotion mechanism of aluminum compounds promoted Pt/MCM-41 catalysts is also summarized.

2 Experimental

The preparation, characterization and evaluation of the catalysts were similar to the procedure described previously.[15-17]

2.1 Preparation of Catalysts

MCM-41 (5 g) was shifted to a three-neck flask equipped with mechanical stirrer. Hexane (50mL) was added to disperse the MCM-41. H_2PtCl_6-ethanol solution containing 0.05 g Pt (0.01g Pt/g MCM-41) was added to the slurry under stirring. The slurry was maintained at 75 ^oC for 1 h, and then hexane was vaporized under a nitrogen stream (200 mL/min). After the support of platinum, another 50 mL hexane and required amount of $Al(CH_3)_3$ solution was added and maintained at 75 ^oC for 1 h, then the solvent was vaporized under nitrogen stream again. The obtained powder was pressed and sieved into 16~20 mesh grain. Finally, the sample was dried at 110 ^oC for 2 h and calcinated at 400 ^oC for 4 h. The obtained catalysts were labeled as Pt-xAl, where x = 0, 5, 10, 15 or 20 denoted the Al/Pt mole ratio.

2.2 Characterization of catalysts

The pore structure and specfic surface area of the catalysts were measured by nitrogen adsorption-desorption isotherms on a Micromeritics TriStar 3000 analyzer at -196 ^oC. The multi-point Brumauer-Emmett-Teller (BET) method was used in the calculation of specific surface area and the Barrett-Joyner-Halenda (BJH) model is used in the calculation of average pore size and total pore volume.

The crystal structure of the catalysts were characterized by powder XRD patterns on a Rigaku D/Max 2500 instrument with Cu Kα radiation (λ = 0.1541 nm) operated at 40 kV and 200 mA. Spectra were collected in the 2θ range 30^o~90^o.

The morphology and size of platinum particles were observed on a JEM-2100F transmission electron microscope (TEM) at 200 kV.

The NH_3-TPD profiles were obtained on a Quantachrome ChemBET TPR/TPD chemisorptions flow analyzer from 80 ^oC to 600 ^oC at a ramp rate 15 ^oC/min in He atmosphere.

The Py-FTIR and CO-FTIR spectra were recorded on a Bruker Vertex 70 FTIR spectrometer in transmision model with a resolution of 4 cm^{-1}. Self-supporting wafers of catalyst was placed into an IR cell with CaF_2 windows, in-situ reduced with H_2-N_2 mixture at 400 ^oC for 0.5 h (50mL/min, 5% of H_2, ramp rate 2 ^oC/min), and then evacuated at 400 ^oC for 1 h. Then sample was cooled to 100 ^oC and 30 ^oC before being exposed to pyridine vapor and CO, respectively. The Py-FTIR spectra were recorded after being degassed at 150 ^oC and 280 ^oC for 0.5 h. The CO-FTIR spectra were recorded after exposed to 2500 Pa CO for 30 min and evacuated at 0.01 Pa for 20 min.

2.3 Catalyst evaluation

Catalytic activity and sulfur-tolerant evaluation were performed on a continuous down-flow fixed bed reactor. Catalyst was loaded in the isothermal zone of the fixed bed reactor and in-situ reduced with 120 mL/min H_2 at 400 ^oC for 4 h (ramp rate: 2 ^oC/min). Reaction temperature and pressure are 280 ^oC and 5 MPa, respectively. Tetralin (20 wt.%)-*n*-dodecane solution was supplied by a Series II piston pump at 0.3 mL/min (0.26 g/min, WHSV = 52 h^{-1}). Hydrogen flow rate is 120 mL/min. Tetralin (20 wt.%)-*n*-dodecane solution with 300 ppm of benzothiophene (72 ppm of sulfur) was used for the sulfur-tolerance evaluation. The products were quantitative analyzed on an Agilent 7890A GC equipped with an HP-PONA capillary column (50m×0.2mm×0.5μm) and an FID detector.

3 Results

3.1 Textural properties of the catalysts

Table 1 lists the textural properties of the catalysts. The specific surface area, pore diameter and pore volume are similar to that of the MCM-41 support.

Table 1. Textural properties of the reduced catalysts

Catalyst	Al/Pt	Si/Al	S, m^2/g	D_p, nm	V_p, cm_3/g	$d_{Pt, XRD}$, nm	$d_{Pt, TEM}$, nm
MCM-41	---	---	912	3.89	1.04	---	---
Pt-0Al	0	∞	813	3.95	0.96	6.4/5.3	4.0
Pt-5Al	5	64	882.9	3.80	1.03	6.0/3.4	3.1
Pt-10Al	10	32	875.1	3.78	1.02	5.8/4.6	2.9
Pt-15Al	15	21	858.8	3.85	1.03	6.4/5.1	3.5
Pt-20Al	20	16	839.4	3.89	1.01	6.6/5.1	---

S: specific surface area; D_p: pore diameter; V_p: pore volume; $d_{Pt, XRD}$: (111)/(200) face platinum particle diameter from the XRD line broadening using the Scherrer formula; $d_{Pt, TEM}$: average diameter of platinum particle from TEM photograph.

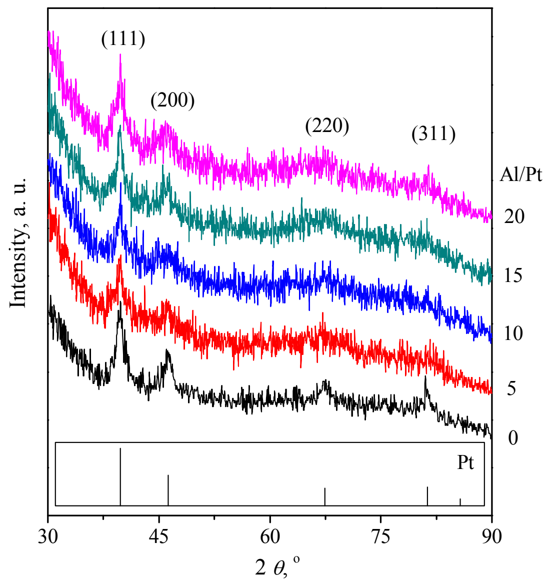

Fig. 1 XRD patterns of the catalysts

Fig. 1 shows the XRD patterns of the catalysts in 2θ = 30.0^o~90.0^o range. The standard PDF card is drawn at the bottom of the figure. The face-centered cubic platinum (0) particle is detected in the catalyst. The well dispersion of platinum in catalysts is indicated by the broadening of diffraction peak . The average sizes of nano-platinum particles are estimated from (111) and (200) peaks using Scherrer formula. The results are also

This journal is © The Royal Society of Chemistry [year]

RSC Advances Accepted Manuscript

listed in Table 1. The nano platinum particles can also be observed directly by TEM (Fig. 2). It can be found that size of Pt particles increase first and then decrease with the increase of Al/Pt ratio. The Pt-10Al catalyst possesses the smallest platinum particles.

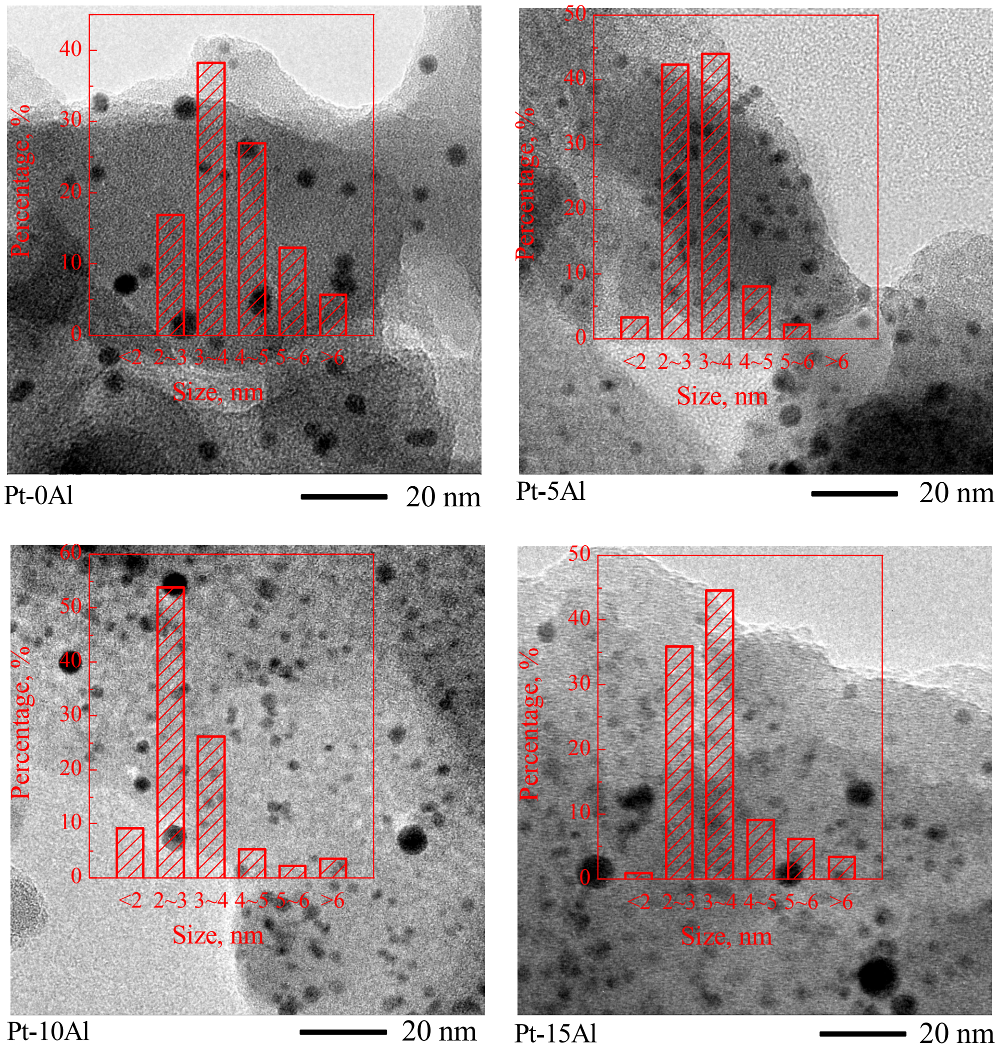

Fig. 2 TEM micrograph and platinum particle size distribution of the catalysts

3.2 Acidity of the catalyst

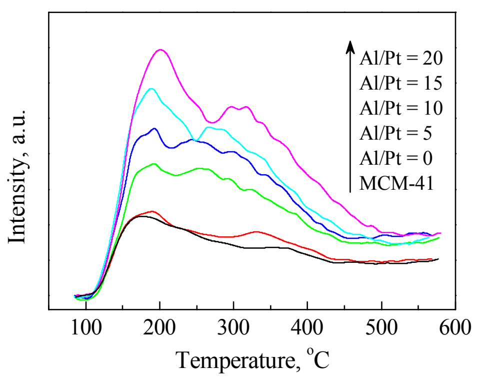

Fig. 3 The NH_3-TPD profiles of the support and catalysts

The acidities of the catalysts are investigated by NH_3-TPD and Py-FTIR. Fig. 3 shows the NH_3-TPD profiles of the catalysts. The NH_3 desorption peak below 300 °C which can be observed on all catalysts and the MCM-41 support is ascribed to hydrogen-bonded NH_3 on silanol.[18, 19] The NH_3-TPD profile of Pt-0Al catalyst is similar to that of MCM-41, but a little more high signal above 300 °C. The difference indicates platinum and residue chlorine cause a small amount of acid site. As indicated by the signal intensity, the amount of acid site increases with the increase of Al/Pt.

Fig. 4A and 4C shows the Py-FTIR spectra of the catalysts. The bands at about 1445 and 1595 cm^{-1} indicate the silanol or hydroxyl group; 1453, 1575 and 1619 cm^{-1} indicate the Lewis acid site while 1542 and 1637 cm^{-1} indicate the Brönsted acid site. The peak at 1489 cm^{-1} is contributed by three types of adsorption sites.[19-21] The Al-free catalyst show some silanol bonded pyridine

RSC Advances Accepted Manuscript

(1445 and 1595 cm^{-1}) and very little Lewis and Brönsted acid sites. While $Al(CH_3)_3$ is added, it reacts with the surface silanol and grafts onto the MCM-41. At low Al/Pt ratio (Al/Pt = 5), the Al-CH_3 bond may be hydrolysed which leads to more hydroxyl-aluminium, as indicated by the increase of peaks at 1445 and 1595 cm^{-1}. With the increase of Al/Pt ratio, the adjacent hydroxyl-aluminium dehydrates and results in the formation of Lewis and Brönsted acid. Meanwhile, the amount of hydroxyl is decreased. This is indicated by the shift of 1445 cm^{-1} peak to 1453 cm^{-1} and the increase of peaks at 1489, 1542, 1619 and 1637 cm^{-1}.

Fig. 4B and 4D shows the amount of acid sites. The values are calculated with the method provided by Emeis.[22]

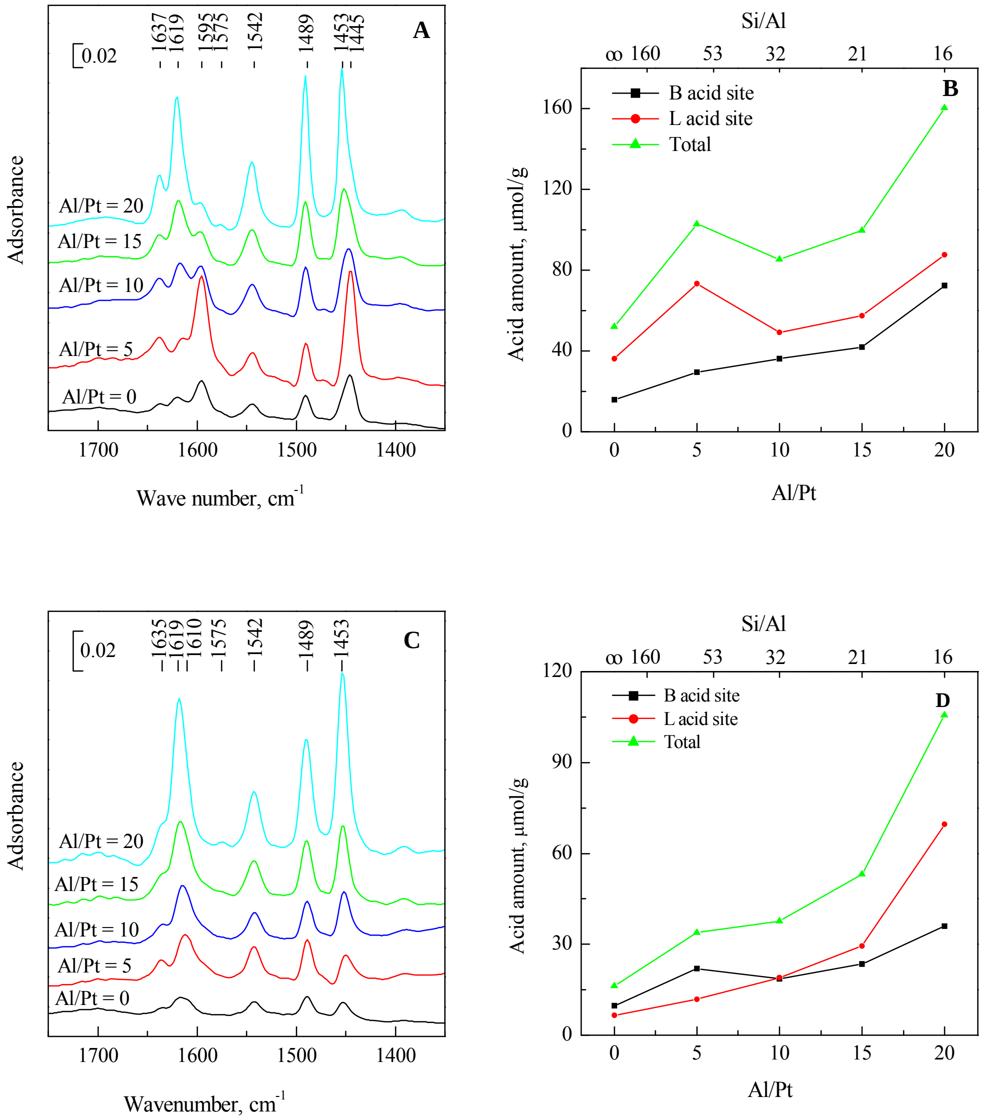

Fig. 4 Py-FTIR spectra and acid amount of the catalysts. A and B: 150 °C, C and D: 280 °C.

3.3 FTIR spectra of adsorbed CO

The FTIR spectra of adsorbed CO are collected to investigate the properties of nano-platinum particles (Fig. 5). Two absorbance bands can be ascribed to CO adsorbs on zero-ordered platinum atoms: the one at about 2080 cm^{-1} is attributed to the CO linear bonding to platinum (Pt^0-CO) and the other one between 1800 and 1900 cm^{-1} is attributed to the CO bridged adsorbing on platinum (Pt^0-CO-Pt^0).[13, 23-26] The peak areas, which are related to the amount of adsorbed CO and roughly reflect the amount of accessible platinum atoms[27, 28], are listed in Table 2. Peak positions are also listed. With the increase of Al/Pt ratio, The area of linear bonded CO band increases at low Al/Pt ratio and than decreases while the Al/Pt ratio is further raised. The catalyst with an Al/Pt = 10 has the best Pt dispersion, which is consistent with XRD and TEM results. There are more defect Pt atoms (corner, edge and kink sites) in well dispersed catalyst and the defect platinum atom brings in the low vibration frequency of linear-bonded CO band (Table 3).[29, 30] Hence, the peak position shifts from 2900.69 to 2084.98 and then to 2086.73 cm^{-1} with the

This journal is © The Royal Society of Chemistry [year]
RSC Advances Accepted Manuscript

increase of Al/Pt ratio.

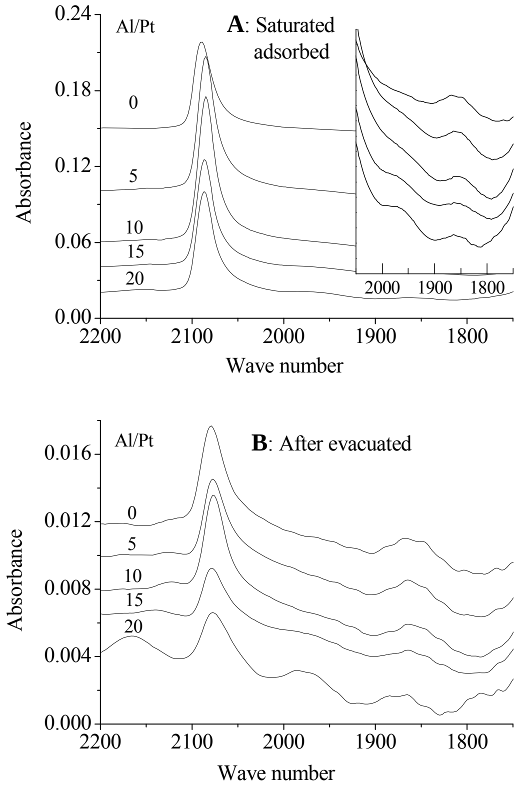

Fig. 5 CO FTIR spectra of the catalysts.

Table 2. Peak position and integrated area of linear bonded CO

Al/Pt	Saturated		After evacuation		Red shift cm^{-1}
	Position	Integrated area	Position	Integrated area	
0	2090.69	2.212	2079.31	0.331	-11.38
5	2085.25	3.484	2079.08	0.216	-6.17
10	2084.98	3.691	2078.36	0.217	-6.62
15	2086.43	2.804	2080.16	0.156	-6.27
20	2086.73	2.641	2079.18	0.173	-7.55

Fig. 5B shows the FTIR spectra after CO evacuation. A very weak shoulder peak at about 2123 cm^{-1} is observed on Al-free catalyst. This peak is shifted to 2124, 2125, 2140 and 2165 cm^{-1} as well as the integrated area increases with the increase of Al/Pt. It is commonly agreed that the band from 2100 to 2170 cm^{-1} can be assigned to the CO bonded to electron-deficient $Pt^{\delta+}$ atoms. [25, 31-33] Moreover, high-frequency bands in the CO stretching region characterizes high electron-deficiency states of platinum. Thus it is reasonable to conclude that the electron density of platinum decreases with the increase of Al/Pt, and the amount of electron-deficient platinum atoms increases as well.

Additionally, a shoulder band can be observed at about 1960 cm^{-1} for catalysts with high Al/Pt ratio. This band may be ascribed to that the interaction between platinum atom and acid site leads to the formation of Pt-carbonyl-hydride ($Pt \langle {}^{CO}_{H}$).[34]

3. 4 Catalytic Performance

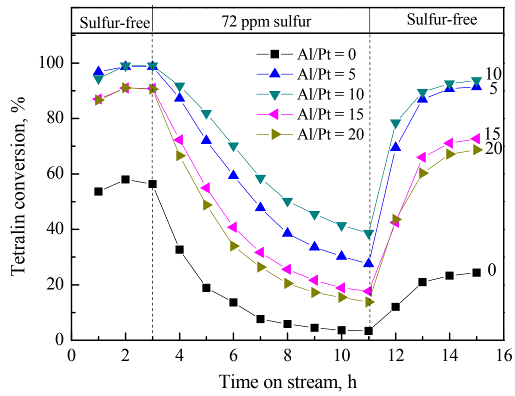

Fig. 6 Tetralin conversion with the presence and absence of 300 ppm benzothiophene (72 ppm sulfur). Reaction conditions: 280 °C, 5 MPa, 0.3 g catalyst, 120 mL/min H_2, 0.3 mL/min liquid (52 h^{-1})

Table 3 Pseudo-first-order rate constants of the catalyst at stable state

Al/Pt	reaction rate constants, $\times 10^{-3}\ s^{-1}$			relative rate constant		
	k_1	k_2	k_3	k_1'	k_2'	k_3'
0	11.96	0.49	4.03	1.00	1.00	1.00
5	63.16	4.66	35.51	5.28	9.43	8.80
10	66.67	7.06	39.93	5.57	14.27	9.90
15	34.50	2.81	18.74	2.88	5.69	4.64
20	34.13	2.14	16.78	2.85	4.33	4.16

Note: $k = -\text{WHSV} \ln(1-x)$. k_1: sulfur-free at 3 h; k_2: 300 ppm benzothiophene (72 ppm sulfur) at 11 h; k_3: sulfur-free at 15 h.

Fig. 6 shows the tetralin conversions under sulfur-free and sulfur-containing condition. The pseudo-first-order rate constants ($k = -$ WHSV $\ln(1-x)$) at the stable state (3 h, 11 h and 15 h, k_1-k_3) are listed in Table 3. The relative rate constants are also calculated on the base of the reaction rate constants of Al-free catalyst. The tetralin conversion increases with the increase of Al/Pt at low Al/Pt, and then decreases at high Al/Pt. The catalyst with a Al/Pt = 10 has the best catalytical activity. The pseudo-first-order rate constant of this catalyst is 5.57 times as high as that of the Al-free one under sulfur-free condition. This value comes to 14.27 under sulfur-containing condition. The other Al-containing catalysts are much better than the Al-free one, too. Furthermore, the relative rate constants of Al-containing catalysts under sulfur-containing condition (k_2') and after the sulfur-containing condition (k_3') are much higher than under sulfur-free condition (k_1'), which implies the Al-containing catalysts are much best sulfur-tolerance than the Al-free one.

4 Discussion

Our previous studies have investigations the effects of Al-Pt interaction sequence, Al/Pt ratios of $AlCl_3$ and aluminum promoter type on the performance of Pt-Al/MCM-41 catalysts. The promotion mechanism of aluminum promoters on the properties and performances of Pt/MCM-41 catalysts are discussed and summarized below.

4.1 Catalytic properties

As previouly discussed, Al-promoters have anchor effect,

RSC Advances Accepted Manuscript

isolation effect, and electron-withdrawing effect which affect the fromation of platinum particles. Al-promoters also provide acid sites and hydroxyl groups as well as favour the spillover hydrogen (Fig. 7). [15-17]

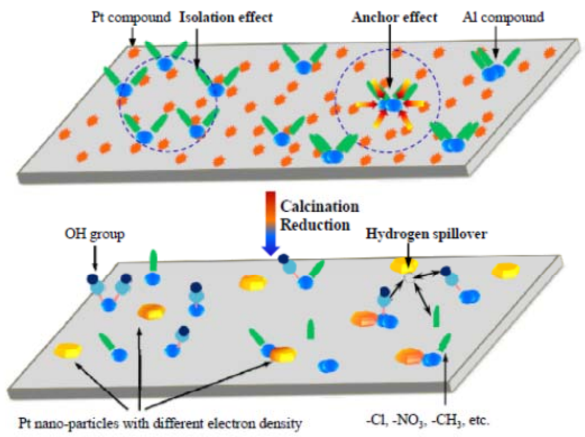

Fig. 7 Interaction mechanism between Al-promoter and Pt.

4.1.1 Isolation and anchor effects and their role on platinum dispertion. The Al-promoters can react with the silanols which are on the surface of MCM-41 and anchor onto the support. [35-37] The anchored Al-promoter likes a barrier which surrounds the platinum compound and confines them in definite region. Hence, the platinum is prevented from sintering and agglomerating and the platinum dispersion is improved. At the same time, the homogeneous MCM-41 surface is destructed by the anchored Al-promoter. The property of aluminum site is more similar to platinum compound than that of silicon site. Thus the platinum compund may be attracted to aluminum sites and anchered onto these sites. Contrasted to the isolation effect, the anchor effect leads to large platinum particle and lows down the platinum dispersion. In the case of specific samples, the effect of Al-promoters can be discussed based on the results of XRD, TEM and CO-FTIR: (1) The attraction effect dominates the platinum particle formation in the sample which $AlCl_3$ is grafted first, thus this catalyst has the lowest platinum dispersion. (2) The reactivity of aluminum compounds decreases in order $Al(CH_3)_3$ > $AlCl_3$ > $Al(NO_3)_3$, thus the $Al(CH_3)_3$ has the best isolation effect while the $Al(NO_3)_3$ has the worst. In consequence, the platinum dispersion is $Al(CH_3)_3$- > $AlCl_3$- > $Al(NO_3)_3$-promoted catalyst at the same Al/Pt ratio. (3) Both isolation and anchor effects are strengthened when the Al/Pt ratio is increased. At high Al/Pt, the $AlCl_3$ and $Al(CH_3)_3$ probable exist as the dimer Al_2Cl_6 and $Al_2(CH_3)_6$. The anchored dimer aluminum have strong attraction effect on platinum which promotes the anchor effect. Thus, the isolation effect dominates at low Al/Pt while the anchor effect dominates at high Al/Pt. As a result, the platinum dispersion increases at low Al/Pt and decreases when Al/Pt is further increased. (4) The $Al(CH_3)_3$ is much more reactivity with silanol than $AlCl_3$ does. For this reason, the isolation effect plays the leading role in a more wide Al/Pt range for the $Al(CH_3)_3$-promoted catalysts. As a result, the optimal Al/Pt of the $Al(CH_3)_3$-promoted catalyst is 10 while the one of the $AlCl_3$-promoted catalyst is 2.

4.1.2 Electron-withdrawing effect and its role on the formation of $Pt^{\delta+}$. The aluminum sites present in the forms of Lewis acid, Brönsted acid or Al^{3+} ion. These sites can withdraw electron from the adjacent platinum and leads to the formation of electron-deficient $Pt^{\delta+}$. The residual -Cl, -NO_3 and –CH_3 in the catalyst may also affect the electron status of the platinum particles. [23, 24] The electron status of the platinum particles is reflected on the band shift of linear bonded CO and the band above 2100 cm^{-1} in CO-FTIR spectra. For the specific samples: (1) The pre-grafted $AlCl_3$ anchors the platinum particle onto it. Thus the platinum particles are more electron-deficient in this catalyst than the one $AlCl_3$ is grafted after the supporting of platinum. (2) $Al(NO_3)_3$ is an electrovalent bond compound in which aluminum behaves as Al^{3+} ion; $AlCl_3$ is a covalent bond compound with electron acceptor chlorine element; $Al(CH_3)_3$ is a covalent bond compound with electron donor methyl group. The electron-withdrawing effect is $Al(NO_3)_3$ > $AlCl_3$ > $Al(CH_3)_3$. Therefore, the electron density of Pt particles in the catalysts should increased in sequence $Al(NO_3)_3$-promoted < $AlCl_3$-promoted < Al-free ≈ $Al(CH_3)_3$-promoted. (3) The electron-withdrawing effect is strengthened when the Al/Pt is increased.

4.1.2 Other effect. The Al-promoters provides Lewis and Brönsted acid sites for the catalyst. [35-37] The acid amount increases with the increase of Al/Pt. The $AlCl_3$ increases the Lewis acid greatly while the $Al(CH_3)_3$ leads to more hydroxyl group at low Al/Pt and great amount of Lewis and Brönsted acid sites at high Al/Pt. Additionally, the dissociated hydrogen from platinum may migrate onto the acid sites. As a result, the hydrogen spillover is enhanced.

4.2 Catalytic performances

Pseudo-first-order rate constants under sulfur-free condition and sulfur-containing condition is ploted with integrated area of linearly bond CO band as abscissa axis in fig. 8.

4.2.1 Catalytical activity. A roughly linear relationship between the logarithmic pseudo-first-order rate constant and the integrated area of linearly bond CO band is observed in Fig.8. Since the area of linearly bond CO band relates to the platinum dispersion, it is undoubted to conclude that the platinum dispersion is the primary factor which determines the activity of the catalyst. [17, 38, 39]

Contrast the catalysts in similar platinum dispersion, it can be found that: (1) the $Al(CH_3)_3$-promoted catalysts have much better catalytic activity than the $AlCl_3$-promoted ones; (2) the $AlCl_3$-promoted ones is better than $Al(NO_3)_3$-promoted one; and (3) the Al-free catalyst is better than $Al(NO_3)_3$-promoted one. Combine with the above discussed electron-withdrawing effect of Al-promoters, it can be concluded that the tetralin hydrogenation is in favour of less electron deficient platinum particles.

Additionally, the acid sites and hydroxyls provide additionally active sites and favour spillover hydrogen which may also contribute to hydrogenation activity. [40, 41]

This journal is © The Royal Society of Chemistry [year]
RSC Advances Accepted Manuscript

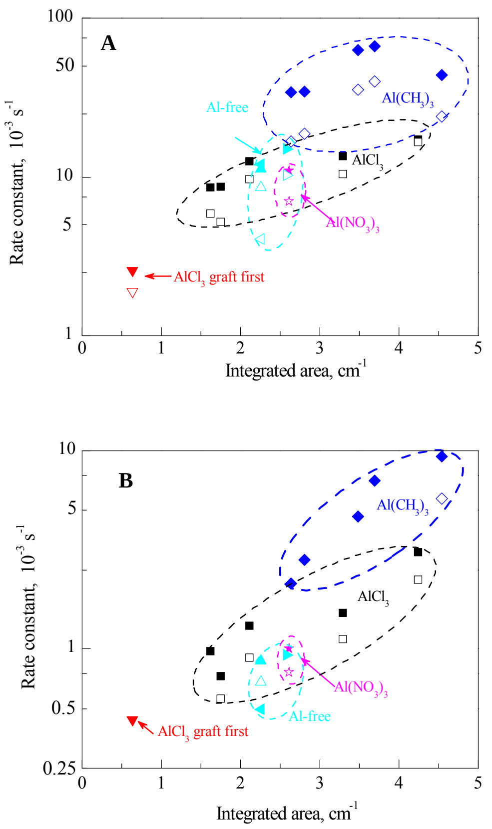

Fig. 8. First-order reaction rate constant of tetralin hydrogenation vs. integrated area of linearly bond CO band. A: sulfur-free condition (solid), sulfur-free after sulfur-containing condition (open); B: with 300 ppm benzothiophene in feedstock (solid: low WHSV, open: high WHSV).

Table 4 The residual benzothiophene (BT) concentration at stable condition

promoter	Al/Pt, mol/mol	BT in product, ppm	promoter	Al/Pt, mol/mol	BT in product, ppm
None [a]	0	39.3	$Al(NO_3)_3$ [c]	2	13.2
$AlCl_3$ [a, e]	0.8	15.4	$AlCl_3$ [c]	2	8.7
$AlCl_3$ [a, f]	0.8	6.3	$Al(CH_3)_3$ [c]	2	4.5
	0	27.2		0	39.8
	1	15.5		5	19.1
$AlCl_3$ [b]	2	8.7	$Al(CH_3)_3$ [d]	10	12.8
	4	15.2		15	13.5
	8	16.6		20	16.3

Detail reaction conditions see: a. ref [16]; b. ref [17]; c. [18]; d. Fig. 6; e. platinum was supported after the grafting of $AlCl_3$; f. platinum was supported before the grafting of $AlCl_3$.

4.2.2 Sulfur-tolerance. As previously discussed, benzothiophene is more competitive adsorbable to the platinum site than tetralin due to its benzenic ring, thiophenic rings and electronegative sulfur atom.[15-17, 42, 43] The deactivation of the catalyst is mainly caused by the competitive adsorption of benzothiophene which hinders the adsorption and hydrogenation of tetralin. Therefore, good sulfur-tolerance can be achieved if the hydrogen desulfurization activity is improved. In other words, the low residual benzothiophene concentration in the product implies the catalyst probable have good sulfur-resistence. The residual benzothiophene concentration at stable condition are listed in Table 4.

The primary factor that determines the sulfur-tolerance of the catalyst is also the platinum dispersion. As it is observed in Fig. 8B, the pseudo-first-order rate constant keeps a increase intendency with the increase of platinum dispersion under sulfur-containing condition. The reason is that high platinum dispersion also provides more activity sites for the both tetralin hydrogenation and benzothiophene hydrogenation. As it is showed in Table 4, the residual benzothiophene concentration is 8.7 at Al/Pt =2 and 12.8 at Al/Pt =10 for $AlCl_3$- and $Al(CH_3)_3$-promoted catalysts, respectively. These two catalysts are also the highest platinum dispersion catalysts for the $AlCl_3$- and $Al(CH_3)_3$-promoted catalysts, respectively.

The electron density of platinum particle also affects the sulfur-tolerance of the catalyst. As it is observed in Fig. 8, the $Al(NO_3)_3$-promoted catalyst and high Al/Pt ratio $AlCl_3$-promoted catalysts, though low or similar pseudo-first-order rate constant as the Al-free catalyst under sulfur-free condition, has a higher pseudo-first-order rate constant than the Al-free catalyst under sulfur-containing condition. Table 3 also shows that the relative rate constants of all Al-containing catalysts under sulfur-containing condition (k_2') and after the sulfur-containing condition (k_3') are much higher than under sulfur-free condition (k_1'). The reasons are that (1) the plarinum particles in Al-containing catalyst are more electron-deficient than those in the Al-free one; (2) the electron-deficient $Pt^{\delta+}$ strengthens the adsorption of electronnegative benzothiophene; and (3) the $Pt^{\delta+}$ pulls the electrons of benzenic ring and thiophenic ring, and thereby destabilizes the rings which promotes the hydrogenation of thiophenic ring and the scission of S–C bond. As a result, high benzothiophene hydrogenation activity is achieved on electron-deficient $Pt^{\delta+}$ catalyst. This point is verified by the residual benzotiophene concentration listed in Table 4. All Al-containing catalysts have much lower residual benzotiophene concentration than the Al-free one. When benzotiophene concentration is brought down, the tetralin hydrogenation activity is improved. In summary, the sulfur-tolerance of the catalyst is in favour of the electron-deficient $Pt^{\delta+}$.[8-10, 15-17]

Additionally, similar to tetralin hydrogenation, benzothiophene can be adsorbed onto the acid sites and hydroxyl sites, and then be hydrogenated by the spillover hydrogen. Therefore, acid sites might also contribute to the sulfur-tolerance of the catalysts.[5, 7, 12, 14, 40, 41]

5. Conclusions

The $Al(CH_3)_3$ promoter affects the platinum dispersion, decreases the the electron density platinum particles, provides additional acid sites and favors the hydrogen spillover which benefit the tetralin hydrogenation activity and sulfur-tolerance of Pt/MCM-41 catalysts. The pseudo-first-order rate constants of the catalyst with a Al/Pt = 10 are 5.57 and 14.27 times as high as that of the Al-free under sulfur-free and sulfur-containing conditions, respectively. The improvement in platinum dispersion, which is mainly attributed to the isolation and anchor effects of Al promoters, is the primary factor that benefits both tetralin hydrogenation performance and sulfur-tolerance of Al-promoted catalysts. The formation of electron deficient $Pt^{\delta+}$, which is

RSC Advances Accepted Manuscript

caused to the electron-withdrawing effects of Al-promoters, enhances the sulfur-tolerance while reduces the tetralin hydrogenation activity to some extent.

Acknowledgements

The authors acknowledge the support of Analysis Center of Tianjin University for the characterization of samples.

References

1. Worldwide Fuel Charter, E. A. M. Association, A. o. A. Manufacturers, E. M. Association and J. A. M. Association, 4th, September 2006.
2. B. H. Cooper and B. B. L. Donnis, *Appl. Catal. A: Gen.*, 1996, 137, 203-223.
3. C. Song and X. L. Ma, *Appl. Catal. B: Environ.*, 2003, 41, 207-238.
4. R. G. Leliveld and S. E. Eijsbouts, *Catal. Today*, 2008, 130, 183-189.
5. S. Nassreddine, S. Casu, J. L. Zotin, C. Geantet and L. Piccolo, *Catalysis Science & Technology*, 2011, 1, 408-412.
6. T. Tang, C. Yin, L. Wang, Y. Ji and F.-S. Xiao, *J. Catal.*, 2008, 257, 125-133
7. S. Nassreddine, L. Massin, M. Aouine, C. Geantet and L. Piccolo, *J. Catal.*, 2011, 278, 253-265.
8. A. E. Coumans, D. G. Poduval, J. A. R. van Veen and E. J. M. Hensen, *Appl. Catal. A: Gen.*, 2012, 411, 51-59.
9. O. Y. Gutierrez, Y. Z. Yu, R. Kolvenbach, G. L. Haller and J. A. Lercher, *Catalysis Science & Technology*, 2013, 3, 2365-2372.
10. K. B. Sidhpuria, P. A. Parikh, P. Bahadur, B. Tyagi and R. V. Jasra, *Catal. Today*, 2009, 141, 12-18.
11. A. M. Venezia, V. L. Parola, B. Pawelec and J. L. G. Fierro, *Appl. Catal. A: Gen.*, 2004, 264, 43-51.
12. S. D. Lin and M. A. Vannice, *J. Catal.*, 1993, 143, 563-572
13. B. Pawelec, R. Mariscal, R. M. Navarro, S. van Bokhorst, S. Rojas and J. L. G. Fierro, *Appl. Catal. A: Gen.*, 2002, 225, 223-237.
14. H. J. Kim and C. Song, *Energy Fuels*, 2014, 28, 6788-6792.
15. M. Luo, Q. Wang, G. Li, X. Zhang, L. Wang and L. Han, *Catal. Commun.*, 2013, 35, 6-10.
16. M. Luo, Q. Wang, G. Li, X. Zhang and L. Wang, *Catal. Lett.*, 2013, 143, 454-462.
17. M. Luo, Q. Wang, G. Li, X. Zhang, L. Wang and T. Jiang, *Catalysis Science & Technology*, 2014, 4, 2081-2090.
18. F. Lónyi and J. Valyon, *Microporous Mesoporous Mater.*, 2001, 47, 293-301.
19. M. C. Kung and H. H. Kung, *Catalysis Reviews*, 1985, 27, 425-460.
20. A. Corma, *Chem. Rev.*, 1995, 95, 559-614.
21. E. P. Parry, *J. Catal.*, 1963, 2, 371-379.
22. C. A. Emeis, *J. Catal.*, 1993, 141, 347-354.
23. R. M. Navarro, B. Pawelec, J. M. Trejo, R. Mariscal and J. L. G. Fierro, *J. Catal.*, 2000, 189, 184-194.
24. S. Albertazzi, G. Busca, E. Finocchio, R. Glöckler and A. Vaccari, *J. Catal.*, 2004, 223, 372-381.
25. K. I. Hadjiivanov and G. N. Vayssilov, *Advances in Catalysis*, 2002, 47, 307-511.
26. P. Hollins, *Surf. Sci. Rep.*, 1992, 16, 51-94.
27. M. A. Albiter and F. Zaera, *Langmuir*, 2010, 26, 16204–16210.
28. R. A. Shigeishi and D. A. King, *Surf. Sci.*, 1976, 58, 379-396.
29. A. Davydov, *Molecular Spectroscopy of Oxide Catalyst Surfaces*, Wiley, 2003.
30. A. A. Solomennikov, Y. A. Lokhov, A. A. Davydov and Y. A. Ryndin, *Kinet. Catal.*, 1979, 589-594.
31. A. Y. Stakheev, E. S. Shpiro, O. P. Tkachenko, N. I. Jaegery and G. Schulz-Ekloffy, *J. Catal.*, 1997, 169, 382–388.
32. V. L. Zholobenko, G.-D. Lei, B. T. Carvill, B. A. Lerner and W. M. H. Sachtler, *J. Chem. Soc., Faraday Trans.*, 1994, 90, 233-238.
33. O. Tkachenko, E. Shpiro, N. Jaeger, R. Lamber, G. Schulz-Ekloff and H. Landmesser, *Catal. Lett.*, 1994, 23, 251-262.
34. A. Erdo˝helyi, K. Fodor and G. Suru, *Appl. Catal. A: Gen.*, 1996, 139, 131-147.
35. Y. Oumi, H. Takagi, S. Sumiya, R. Mizuno, T. Uozumi and T. Sano, *Micropor Mesopor Mat*, 2001, 44, 267-274.
36. S. Sumiya, Y. Oumi, T. Uozumi and T. Sano, *J Mater Chem*, 2001, 11, 1111-1115.
37. J. H. Li, J. A. DiVerdi and G. E. Maciel, *J Am Chem Soc*, 2006, 128, 17093-17101.
38. A. M. Venezia, R. Murania, V. La Parola, B. Pawelec and J. L. G. Fierro, *Appl. Catal. A: Gen.*, 2010, 383, 211-216.
39. Y. Yoshimura, M. Toba, T. Matsui, M. Harada, Y. Ichihashi, K. K. Bando, H. Yasuda, H. Ishihara, Y. Morita and T. Kameoka, *Appl. Catal. A: Gen.*, 2007, 322, 152-171.
40. H. Yang, H. L. Chen, J. W. Chen, O. Omotoso and Z. Ring, *J. Catal.*, 2006, 243, 36-42.
41. F. Roessnera and U. Roland, *J. Mol. Catal. A: Chem.*, 1996, 112, 401-412
42. V. G. Baldovino-Medrano, P. Eloy, E. M. Gaigneaux, S. A. Giraldo and A. Centeno, *J. Catal.*, 2009, 267, 129-139
43. F. Besenbacher, M. Brorson, B. S. Clausen, S. Helveg, B. Hinnemann, J. Kibsgaard, J. Lauritsen, P. G. Moses, J. K. Nørskov and H. Topsøe, *Catal. Today*, 2008, 130, 86-96.

RSC Advances Accepted Manuscript

This journal is © The Royal Society of Chemistry [year]